



ÉCOLE POLYTECHNIQUE FÉDÉRALE DE LAUSANNE

MASTER THESIS - CREATE LAB
FINAL REPORT

SPATIALLY DISTRIBUTED FORCE SENSING
INTEGRATION IN A BIO INSPIRED ROBOT HAND

By:
Selina BOTHNER - 284028

Supervisor:
Kai JUNGE

Professor:
Josie HUGHES

Spring semester 2024

Contents

1	Introduction	2
2	Methods	5
2.1	Sensors	5
2.2	Silicone moulding	6
2.3	Designs	7
2.4	Version 1	7
2.4.1	Version 2	8
2.4.2	Full hand version	10
2.5	Experimental setups	11
2.5.1	UR5 probe test	11
2.5.2	Single finger setup	11
3	Results	14
3.1	Spatial resolution	14
3.2	Repeatability	14
3.3	Object orientation	17
3.4	Skin sensitivity	17
3.5	Full hand	19
4	Discussion	20
5	Bibliography	21

1 Introduction

Sensing is a crucial aspect of robotic manipulators as it enables a system to interact intelligently with its environment through the ability to detect contact, temperature, humidity, and more. These capabilities are essential for a system to adapt to its surroundings, allowing it to perform task more effectively and safely. Moreover, sensing can also provide data that serves as feedback in a control loop, enhancing the precision and smoothness. Force sensing is essential as it enables the hand to detect objects and measure the applied force for tasks requiring precision and delicacy through controlling the grip strength. Additionally, force sensing provides real-time feedback, allowing for fine-tuned movements and ensuring a stable and secure grip. Incorporating force sensors enhances the robotic hand's dexterity and adaptability, making it more effective in various applications.

The integration of sensing capabilities in anthropomorphic robotic hands pose a unique challenge due to its mechanical complexity. Constrained to the size of a human hand, integrating actuation and sensing, while keeping a compact form is a significant challenge. One must take into account the size and the weight of sensors to avoid disrupting the hand's movements. Ensuring the optimal spatial distribution of sensors adds another layer of difficulty, as sensors must be strategically positioned to provide full sensor coverage without interfering with the rest of the system. Despite the limited space available, one must find ways to effectively incorporate the sensors without compromising the hand's functionality. Additionally, the presence of deformable skin on some robotic hands further complicates sensor integration.

This thesis focuses on integrating spatially distributed force sensing in an existing bio-inspired robotic hand: ADAPT Hand2. The ADAPT Hand2 consists of a 3D-printed palm and five fingers, controlled by tendons actuated by motors and with a silicone skin covering the full surface.

As force sensing is such a crucial part of robotics, many methods have been developed to do this. For example, Force Sensitive Resistors (FSR) (as in [1]) can be used. These sensors change resistance when a force is applied to it. While these are quite cheap, their form factor makes them difficult to integrate in a hand. The presence of skin makes their integration even harder. Others, such as the authors in [2], have been able to develop flexible tactile sensors, that are embedded in silicone. However, this method requires a lot of post-processing of the signal. In [3], the authors use a distributed tactile sensor that covers the fingers and the palm. It is however composed of 624 points, making processing and understanding the data challenging. There are also vision-based tactile sensors that use visual perception techniques to precisely detect fingertip contact information [4] and [5]. However, as we are aiming for spatially distributed force sensing, this becomes very challenging to integrate.

Many examples of sensor integration in robotic hands can be found in the literature. A table (Fig 1) summarises their results. However, these implementations have limitations. For instance in [6] and in [7] the authors focus on the development of sensors in the fingertips (with [7] adding temperature sensors), leaving a large portion of the finger sensorless.

In [3], the authors have successfully implemented many sensors across the entire hand, but the design lacks a skin.

The approach in [8] uses a combination of Hall sensors and magnets embedded in the skin to create a force-sensing module strategically placed on the fingers. However, this design involves many wires,

and although dimensions are not specified, the hand appears bulky.

The solution proposed in [9] consists of 3D printed flexible chambers. When a force is applied to these chambers, the pressure will increase and can be detected. However, this design likely cannot determine the force's orientation.

Name	Gifu hand II [3]	SKKU hand II [1]	Hall-effect force sensing [4]	Low-cost robotic hand [2]	3D-printed soft robotic hand [5]	Ours
Authors	H. Kawasaki et al.	B. Choi et al.	L. Jamone et al.	D. Lanigan & Y. Tadesse	O. Shorthose et al.	
Sensors	6 axis force sensor on fingertips + distributed tactile sensor with 624 points.	Tactile fingertip sensors.	17 tactile sensing elements (hall sensor + magnet combination).	Temperature and force sensing on the fingertips.	18 sensing regions on fingers and on palm, made of 3D printed soft chambers.	29 sensing elements, along the fingers.
Skin	No	No	Around the force sensing elements	Yes	Made of 3D printed flexible material	Yes
Anatomy	1 thumb + 4 fingers	1 thumb + 3 fingers	1 thumb + 4 fingers	1 thumb + 4 fingers	1 thumb + 4 fingers	1 thumb + 4 fingers
Force orientation	Yes	Yes	Not mentioned	Yes	No	Yes

Fig. 1: Table summary of the state of the art on hands with sensors

This thesis aims to explore the integration of spatially distributed tactile sensing in the ADAPT Hand2 through three directions. The first is the mechatronics design which allows for sensor integration without compromising the form factor and range of motion of the hand. The second is an experimental validation on a single finger to decouple contact from finger motions and to improve the repeatability. The third is to integrate the sensor on all five digits of the hand.

This report will demonstrate the feasibility of using a combination of hall effect sensors and magnets embedded in a silicone skin to detect whether a finger is in contact with objects. The deformation of the skin through external contact causes a displacement in the magnet position leading to sense the force. The general integration of the hall sensors is performed through a flexible PCB which spans the backside of the finger, with two or more sensors per phalanges. This design allows for scalable electronics readout while maintaining the form factor and motion of the fingers (see Fig.2a and b). The design, fabrication, and mounting of the silicone skin affects the motion/contact decoupling and repeatability of the sensors, and is validated experimentally. Finally, as shown in Fig.2c and d, the five digits are mounted with the fabricated sensor and skin to demonstrate the sensing capabilities across the full hand.

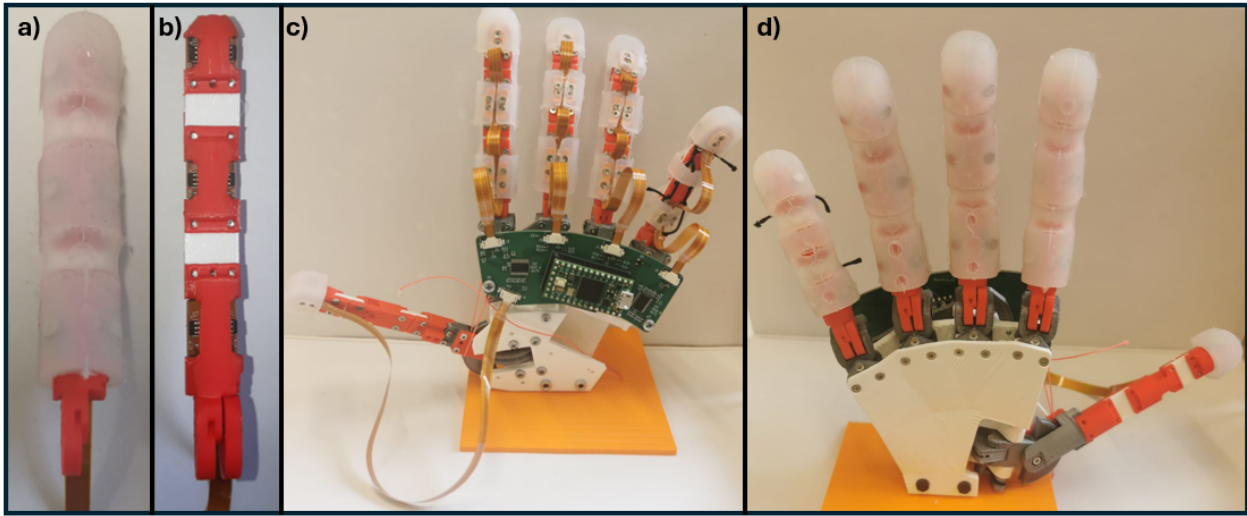


Fig. 2: Pictures of the full hand from the front and back (left) and pictures of the finger with and without the skin (right).

2 Methods

This section covers the fabrication process, beginning with the force sensing concept and the electronics. It then details the silicone moulding and finger designs and concludes with an explanation of the experimental setups.

2.1 Sensors

To embed force sensing in the ADAPT Hand2, a method similar to the one presented in [8] was chosen. Hall sensors are placed within the 3D-printed skeleton of the fingers, and magnets are embedded in the skin. When a force is applied on the skin, it deforms, causing the magnets to move and the hall sensors to detect a change in the magnetic field.

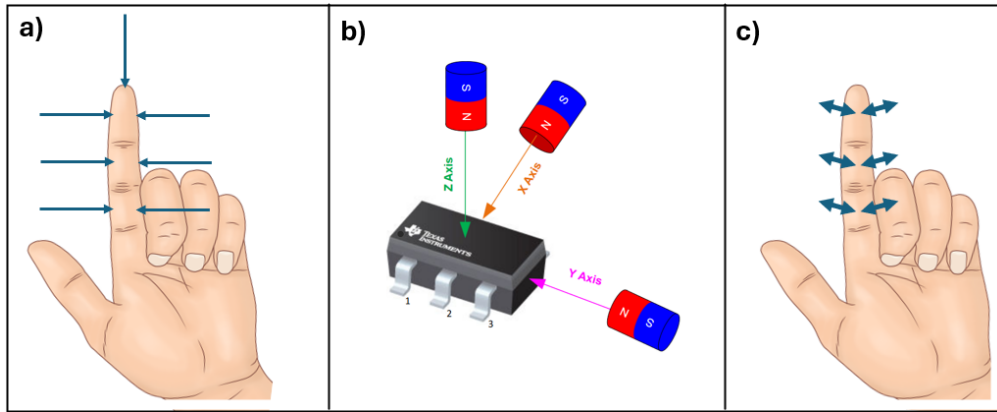


Fig. 3: a) Sensor placement on the index finger. b) Axes of the hall sensor (screenshot from [10]). c) The arrows show the X axis of the sensor with respect to the finger. For the top sensor, the axis correspond to the axis perpendicular to the image.

The TMAG5273 3-axis hall sensor and magnets with a 4mm diameter and 1mm height were chosen to implement these force sensing elements. With this magnet size, the hall sensor values are roughly in the middle of their sensing curve when the magnet is about 3mm above the sensor. This is the ideal placement in the skin as it is far enough for the hall sensor to detect the magnet movement, without leading to too big fingers. Due to the tendons passing through the centreline of the finger, the magnets and the hall effect sensors are placed on the side. As embedding the hall sensors requires removing a part of the 3D-printed bone structure, it is only possible to do this on the sides of the finger, as shown in Fig 3a. To minimize the number of wires and to achieve a cleaner result, the hall sensors are soldered onto a flexible PCB which extends from the back of the hand, up the finger, and wraps around it. This positions the sensors on the front of the finger, angled sideways at 50 °. See Fig 5b and Fig 5c for the CAD (Computer Aided Design) models of the finger and the flexible PCB.

The flexible PCB is connected to the main PCB through a Zero Insertion Force (ZIF) connector. The main PCB also houses a Teensy 4.0 microcontroller, allowing the user to access the hall sensor data. The TMAG5273 exists with 3 different I2C addresses. Modifying the I2C address is possible, but needs to be done at every power up, and requires each sensor to be powered individually (by an

IO pin for example). In the case of our flexible PCB, this would require 8 connection pins between the finger and the main PCB. This can be reduced to 7 by using the TCA9548APWR I2C multiplexer, and using 2 I2C busses and 1 IO pin for each finger. The IO pin powers one hall sensor, in order to change its address. The first I2C bus has 3 sensors (each with their individual and different addresses), and the second has 4 sensors: 3 with their original and individual I2C address, and the sensor with the modified address. With only one finger, both solutions are possible, but this is not scalable to the whole hand. Connecting all the hall sensors of the hand to IO pins to modify their address would require 26 IO pins.

Hall sensors are very sensitive devices. Since the silicone skin of a hand is deformable and does not always return exactly to its initial position the code compensates by memorizing the initial sensor values upon startup and using differential values to compute subsequent readings. Testing showed that the most reliable and repeatable axis was the X axis (Fig 3b), which will be used throughout this thesis. Fig 3c, shows the X axis of each sensor, with respect to the finger. For the top sensor, the X axis is perpendicular with the image.

2.2 Silicone moulding

To design a skin with the correct magnet placement, 3D-printed silicone moulds and inserts were designed. These moulds were crafted for easy pouring and disassembly. The skin design includes small holes allowing easy magnet insertion, and ensuring they stay in place when the skin is put around the finger (Fig 4a). To insert a magnet, one must simply stretch the silicone (red arrow in Fig 4a), and then push the magnet in (blue arrow in Fig 4. a). When the skin is relaxed, the insertion hole prevents the magnet from falling back out. Fig 4b provides an example of an insert used for the skin design, featuring protrusions that create the cavities for the magnets once the skin is cured.

An example for the process to make a silicone skin is explained in Fig 4c. In this example we examine the process for the skin of the first version of the finger. The outer mould consists of 2 3D-printed box parts that are assembled together with screws. Liquid silicone is then poured in the assembled box, filling it about halfway. A 3D-printed insert is placed into the silicone-filled mould. This insert can be seen in more detail in Fig 4b. A fixation bar ensures the insert is correctly positioned and holds it while the silicone cures. After approximately three hours, the skin is ready. The mould is disassembled by removing the top fixation and unscrewing the box parts, allowing the skin to be gently extracted.

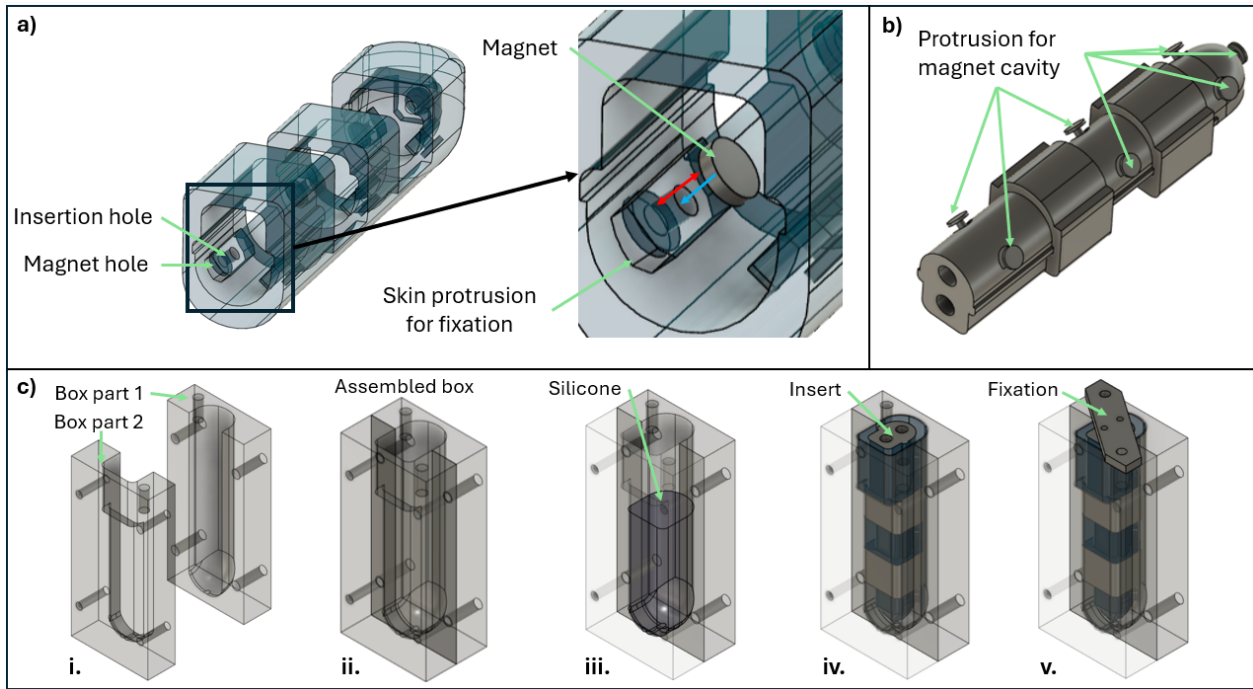


Fig. 4: a) CAD of silicone skin showing the cavities for the magnets. In the zoomed image, the skin must be stretched (red arrow) to insert the magnet (blue arrow). b) 3D printed insert used for the silicone mould, with protrusions that form for the magnet cavities. c) Example process for making the silicone skin. These images correspond to the mould for the version 1 of the finger.

2.3 Designs

2.4 Version 1

Initially, only one finger was designed and manufactured in order to test the design, before equipping the full hand. This version was designed by modifying the existing index finger of the ADAPT Hand2. Slits were incorporated to embed the flexible PCB and its sensors inside (Fig 5a and b). Tabs were added on the sides of the finger to secure the silicone skin and prevent it from moving along the finger (Fig 5a). Additionally, skin protrusions (Fig 4a) are added so the skin blocks on around the slits designed for the flexible PCB.

Once the PCB is inserted into the slits, the silicone skin can be places on top, in the same way one would put on a sock on (Fig 5c). The silicone skin has 7 cavities for magnets, aligning them directly in front of their respective hall sensor. The final assembly is shown in Fig 5d.

In this design the skin shape around the finger joints is flat (Fig 6).

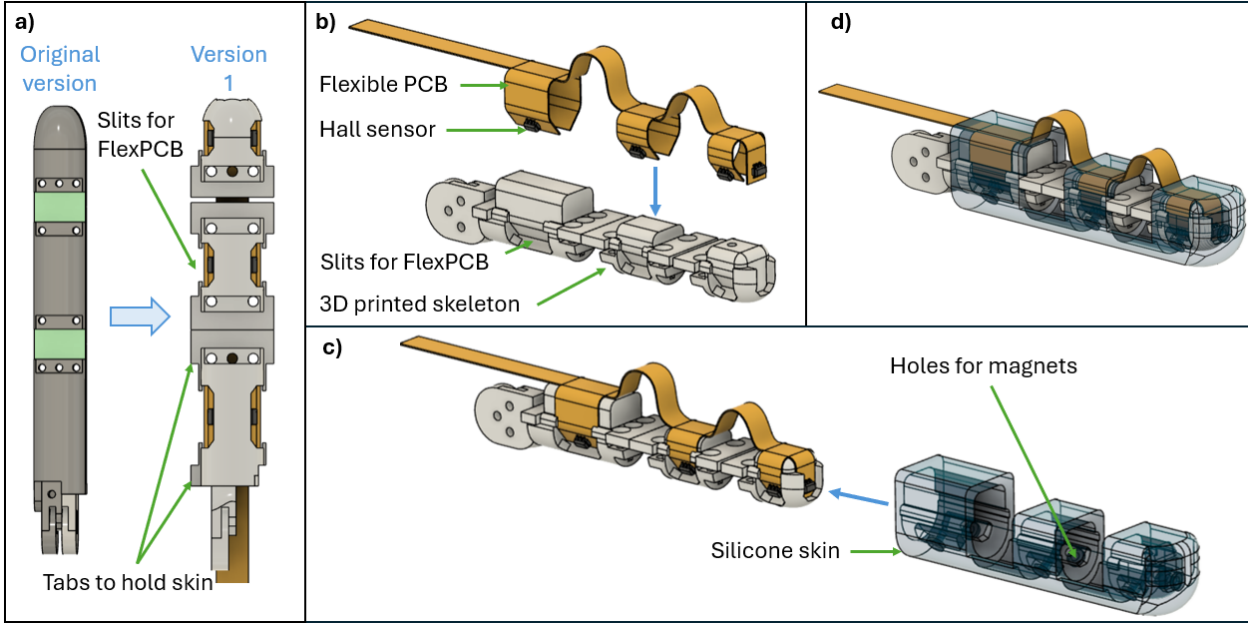


Fig. 5: a) CAD model of the original finger (left) and CAD model of version 1 of the finger with its sensors (right). The main modifications are the slits for inserting the flexible PCB, and the tabs that secure the skin, preventing it from moving along the length of the finger. b) CAD model of the flexible PCB and the 3D-printed bone structure. c) Finger with integrated PCB, and silicone skin with holes for placing the magnets. d) CAD assembly showing the 3D-printed bone structure, flexible PCB, and silicone skin.

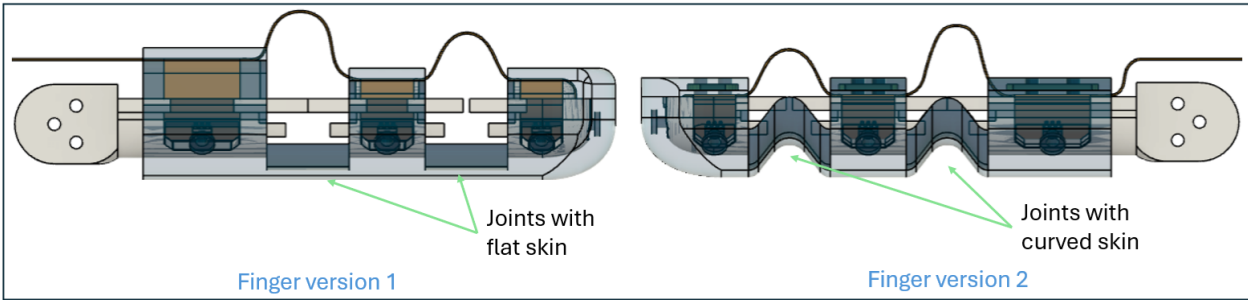


Fig. 6: Left: Finger version 1 with straight skin at the joint. Right: Finger version 2 with bent skin at the joint.

2.4.1 Version 2

The second version of the finger has a more complex structure and fabrication process, but the skin, PCB, and the bones are better secured. The 3D-printed skeleton parts were modified by removing the tabs used to keep the silicon in place, and M2 screw holes were added in the back. This allows the PCB and the skin to be screwed in (Fig 7a). The back was also flattened and made slimmer for

aesthetic reasons.

To anchor the silicone to the skeleton, skin holders are 3D printed and are placed in the silicone mould, so the silicone can set around it (Fig 7b).

Fig 7c shows the flexible PCB wrapped around the 3D-printed skeleton, as well as the skin with its holders.

Instead of wrapping the skin around the skeleton like a sock as in version 1, the top part of the skin now simply covers the top of the finger, while the middle and bottom parts wrap around it from the front. Once everything is assembled, M2 screws secure all components in place as shown in (Fig 7d).

Despite these fixations on the back of the finger, the silicone skin needs to be glued to ensure it remains in place after grasping objects. The placed were the glue is placed can be seen of Fig 7e.

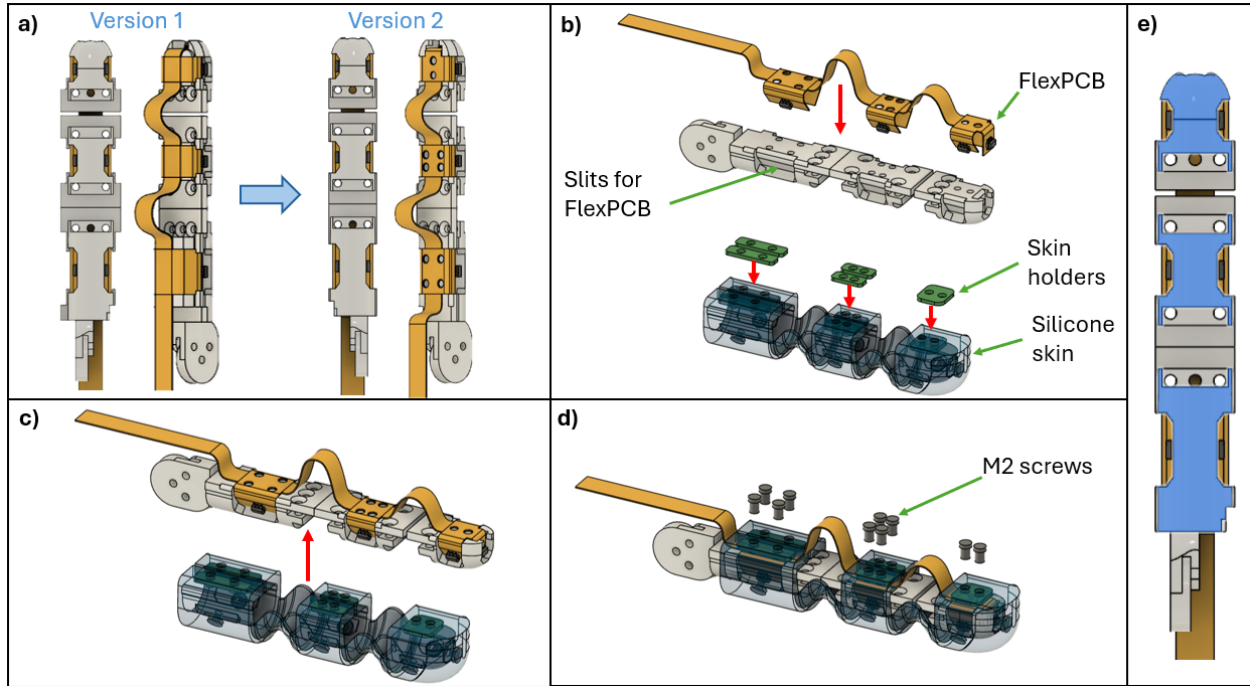


Fig. 7: a) CAD model of version 1 of the finger with sensors (left) and CAD model of version 2 with sensors (right). b) CAD model of the flexible PCB, the 3D-printed bone structure, the silicone skin and the sin holders. c) Assembly of the flexible PCB with the 3D bone structure, and assembly of the skin with the holders. d) CAD assembly showing the 3D-printed bone structure, flexible PCB, silicone skin, the skin holders and the screws to anchor all the elements. e) In blue are the areas where a bit of glue must be added.

In this second version, the skin shape around the finger joints is curved, in order to avoid the skin from bunching up when bending the finger (Fig 6).

Casting the skin holders into the silicone makes the design for the silicone mould quite a bit more complex. Fig 8 shows the CAD of this new mould. To assemble it, the two bottom parts of the

box are put together. Screws go from the bottom of the box, through the skin holders and into the insert, which allows for the correct placement of the skin inserts. The top parts of the box can then be screwed to the bottom part. The silicone is poured through the 5 holes at the top of the design. After curing, the mould is disassembled to release the skin.

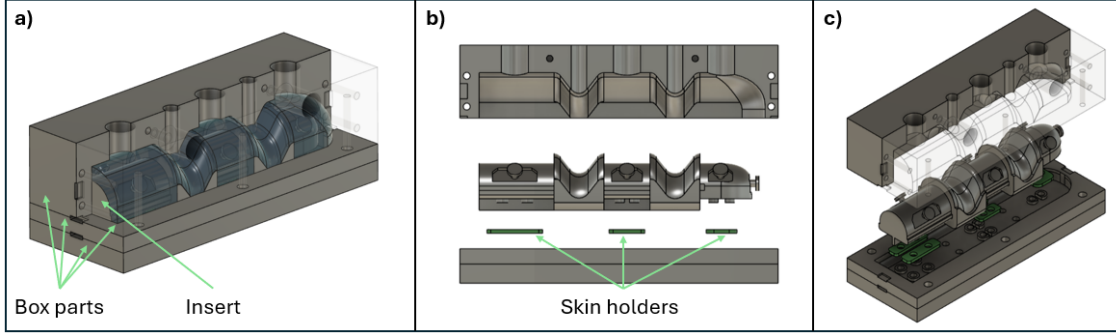


Fig. 8: *CAD of silicone mould for finger version 2 from different angles.*

2.4.2 Full hand version

The design of the full hand is based on the design of version 2. Each fingers follow a similar design (holes in the back for fixation, and the skin is glued to the front of the skeleton), except for the pinky and the thumb that have less sensors. The pinky is missing two sensors in the middle due to insufficient space in the link. The thumb only has sensors on its tip, because it's tendon routing is more complicated and thus requires more space inside the finger, leaving less space for the sensors. The main PCB was also redesigned to accommodate multiple flexible PCBs and to fit the shape of the hand better. The dimensions of the PCB are shown in Fig 9 and the PCBs mounted on the hand can be seen in Fig 2 a and b.

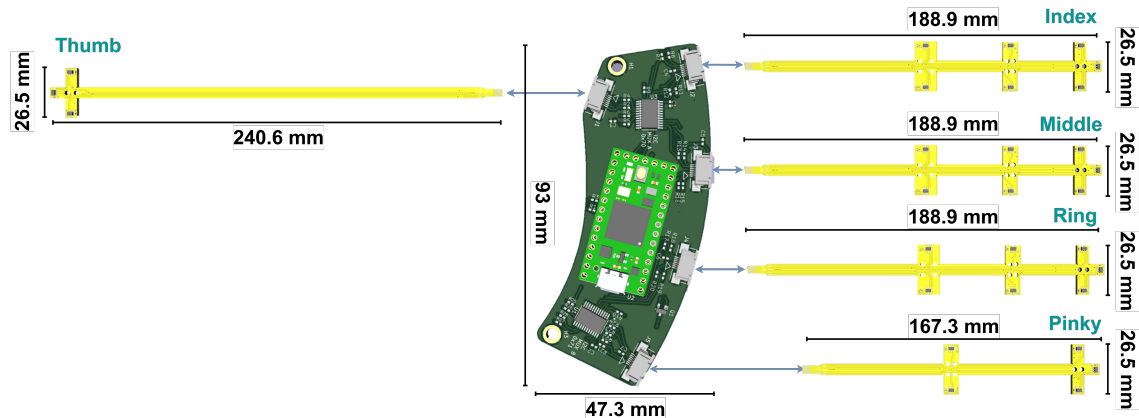


Fig. 9: *All the PCBs and their dimensions. The flexible PCBs are connected to the main PCB through Zero Insertion Force connectors strategically placed to align with their respective finger.*

2.5 Experimental setups

Several experiments were setup during the thesis to assess the functionality and performances of the different designs.

2.5.1 UR5 probe test

The initial test was a probe test using a UR5 robotic arm. In this experiment the finger with the sensors and its skin (version 1) was probed by the robotic arm as an initial test to determine that the force sensing concept works and to gather data on the spatial resolution of the finger sensors. The UR5 robotic arm was equipped with a 6mm diameter probe connected to a load cell, enabling measurement of the probing force. In parallel, the sensor data was recorded. We can then reconstruct the data to determine the force, the sensor values, as well as the probe coordinates. We can then determine the conditions necessary to get useful values from the sensors.

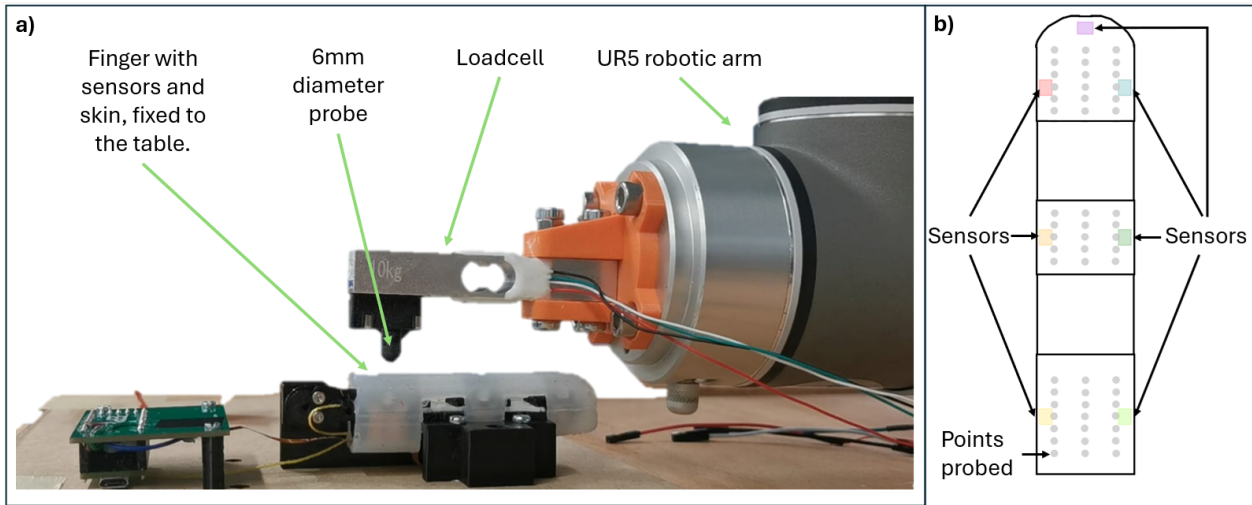


Fig. 10: a) Setup for the probe test with the UR5 robotic arm probing the finger which is fixed to the table. b) Schematic illustrating the probing locations on the finger, with the sensor positions as references.

2.5.2 Single finger setup

Following the probe test, experiments were setup to determine the functionality of the sensors on a finger in motion (Fig 11a). The finger mounted with its sensors and its skin (version 2), where placed on the setup and connected to the motors. The first motor controls the top two axis of rotations (the bending motion of the finger) and the second motor controls the MCP joint (where the finger meets the palm), thus controlling the angle of the finger. These tests focused on sensor readings from the fingertip.

The finger was then used to do two experiments. Firstly, an object was added for the finger to grasp (Fig 11b), in order to determine whether the sensors can detect that the finger is grasping an object based on sensor data.

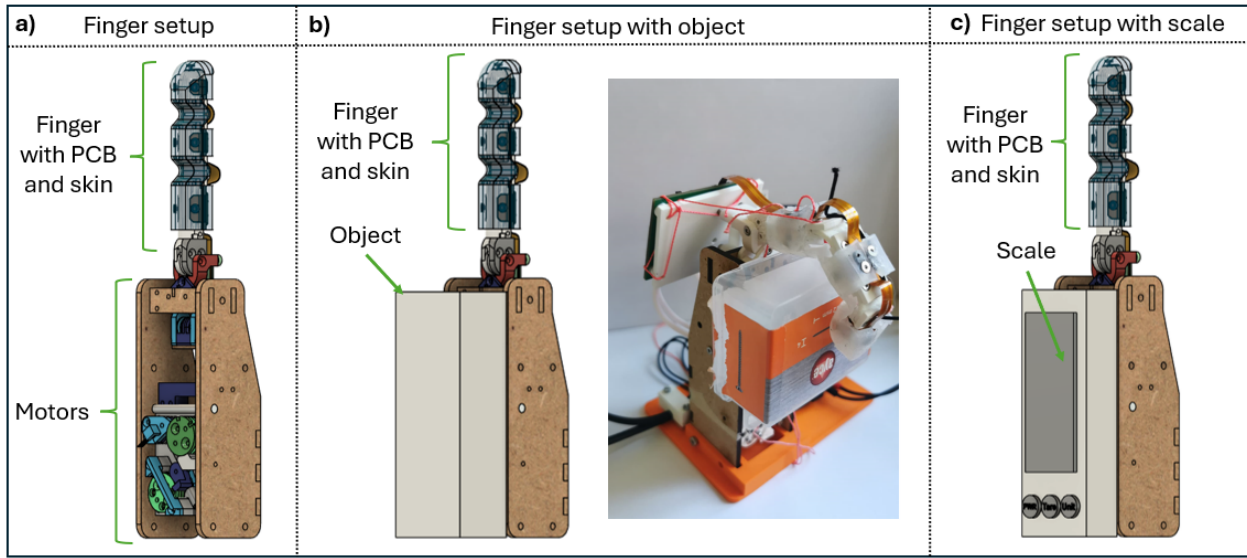


Fig. 11: *Experiments conducted using the single finger setup. a) Single finger setup, with its sensors and its skin. b) Setup to determine sensor response to the presence of an object. c) Setup to determine correlation between force exerted by the finger and sensor values.*

The finger was moved from a straight position into a grasping position five times in a row without an object followed by five times in a row with an object. The sensor's magnitude was measured for each motion. Ideally, the sensor amplitude should be minimal without an object and significantly higher with an object, with consistent results across repetitions. This experiment was tested with 5 different setups:

- finger version 1 with the EF30 silicone
- finger version 2 with the EF30 silicone, with only the screws in the back holding it in place
- finger version 2 with the EF30 silicone, with the screws in the back and glue in the front holding it in place
- finger version 2 with the EF50 silicone, with only the screws in the back holding it in place
- finger version 2 with the EF50 silicone, with the screws in the back and glue in the front holding it in place

The second experiment aimed at determining if the finger was sensitive to the direction of the object. By placing the object with an angle and measuring the sensor response to the finger motion, we determined whether the finger is sensitive to the direction of the object, and thus the orientation of the force applied on its tip. The object was raised by 2cm on one side to do the experiment. This experiment was conducted using the EF30 V2 skin as it gives the best results. Once again, the grasping motion was done 5 times, and the amplitude of the left and right fingertip sensors was analysed.

The final test consists of replacing the object with a scale (Fig 11c), in order to determine whether there is a correlation between the force exerted on the finger and its sensor data.

The finger was set in motion 5 times, initially without touching the scale and gradually applying more force. This experiment was done twice, once with the version 2 of the finger with the EF30 silicone skin, and once with the version 2 of the finger but with the EF50 skin. This experiment aimed to determine the difference in sensitivity of the finger based on the silicone stiffness.

3 Results

3.1 Spatial resolution

The probe test conducted with the UR5 robotic arm provided insights into the spatial resolution of the sensors on the finger. Indeed, from 12 we can see the area that each sensor covers. Of course, this area is dependent on the force applied to the finger and on the size of the object. We can tell that this force sensing method covers all parts of the finger.

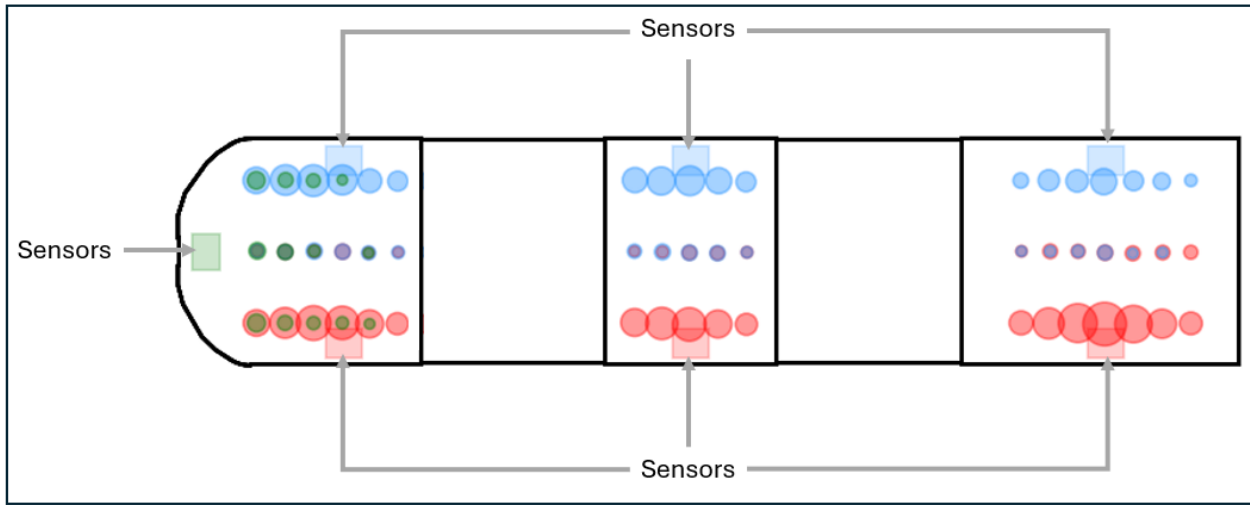


Fig. 12: *UR5 probe test with a 6mm diameter probe. Rectangles indicate the sensor positions. Circles mark the points where the finger was probed, with the circle area proportional to the sensor value at each point. For clarity, only points with sensor values above 1.5mT are shown. This figure illustrates the sensor coverage of the finger.*

When the skin was probed less deeply, resulting in a smaller force applied to the finger, the sensors were still able to detect it, but from a shorter distance. This suggests that the sensors not only provide contact sensing capabilities but also has the potential for measuring force.

3.2 Repeatability

A critical aspect of sensor performance is its repeatability. Consistent data is essential for data processing. This was one of the major challenges of the thesis. Fig. 13 shows the average amplitude of the values measured by the right and left sensors on the tip of the finger, on each bending motion, whether this is with an object (green) or without (blue), for 5 different skin setups.

The results obtained by the EF30 version 1 skin are inconsistent as shown by the large standard deviation (error bars), even without the presence of an object. Furthermore, the results are not very useful as the amplitude measured without an object is higher than the amplitude with one. This indicated low reliability, confirming the need for the second version.

The EF30 version 2 skin without the glue (but with the screws), also showed some repeatability issues, as shown by the large error bars. This means that repeated test yield different results. The same can be said about the EF50 V2 silicone skin without glue (but with the screws), though to a

lesser extent. The reason behind this slightly higher repeatability is likely due to the stiffness of the silicone, allowing it to hold better around the finger and reducing the unwanted movement. When comparing the finger with the EF30 V2 skin glued and screwed, to the EF50 V2 skin glued and screwed, we observed that the EF30 setup had higher amplitudes in the presence of an object, while the EF50 setup had higher amplitudes without an object. This can be explained by the fact that the EF50 skin bunches up a bit more around the joint, due to its stiffness, affecting the sensor readings more when there is no object. However, since the EF30 skin is more sensitive, a greater amplitude is measured in the presence of an object.

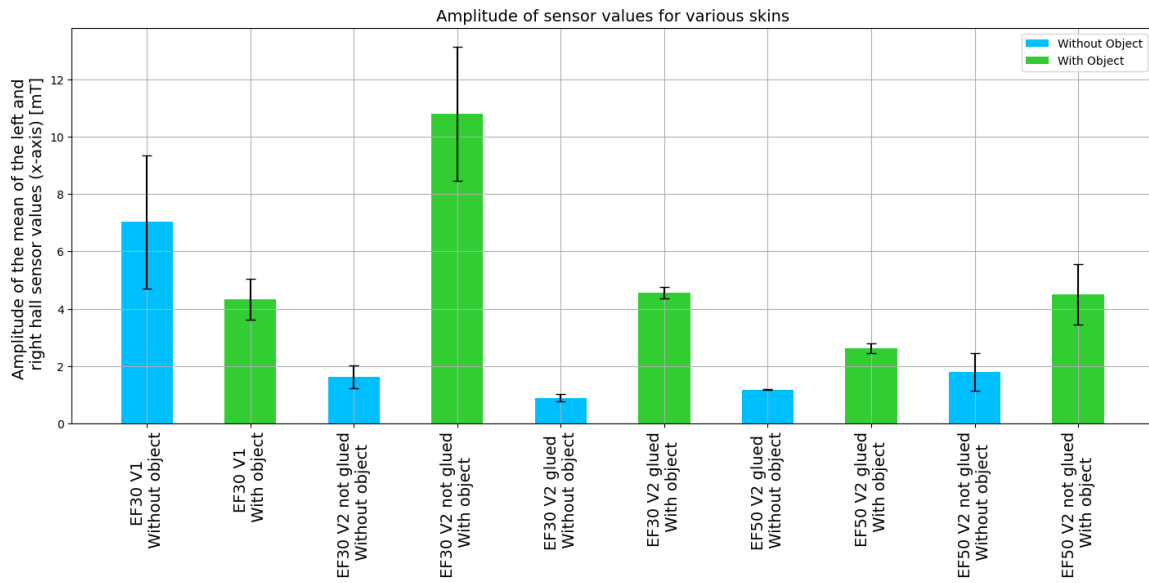


Fig. 13: Bar plot showing the average amplitude of the sensors during the bending motion experiment. In blue are the experiments without the presence of an object and in green are the experiments with an object. The error bars correspond to the standard deviation of the amplitudes observed during the experiment.

These results are further illustrated in Fig. 14 and Fig. 15 which show the best and the worst results respectively. Fig. 14, shows the times series plot with the glued and screwed EF30 V2 skin. On the left, the finger is doing the grasping motion without any object present, resulting in very low sensor readings. On the right, the object is added, resulting in sensor values showing consistent peaks, except for a slight variation in the first one, probably caused by an inexact object placement.

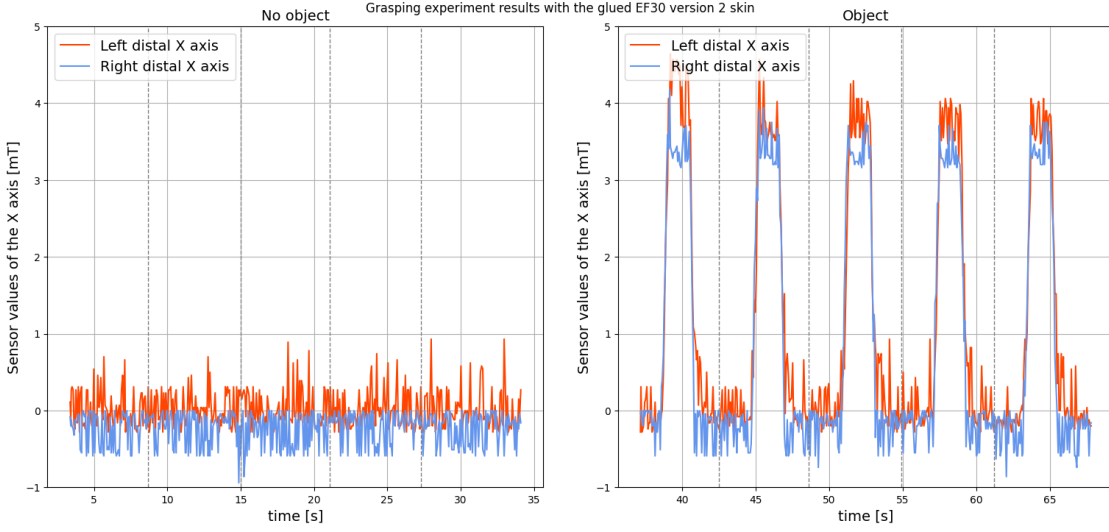


Fig. 14: *Grasping experiment time series using the EF30 version 2 of the skin, with the inside of the front of the skin glued to the finger, and screwed in the back. On the left is the time series without any objects, whilst on the right the object was added.*

In contrast, Fig. 15 shows high sensor values even without an object, as well as drift caused by the finger's motion, causing the magnets to move away from the sensor. When an object is added, the sensor shows lower result, probably indicating that the magnets have moved too far away from the hall sensors. The drift makes the result increasingly inconsistent with each motion.

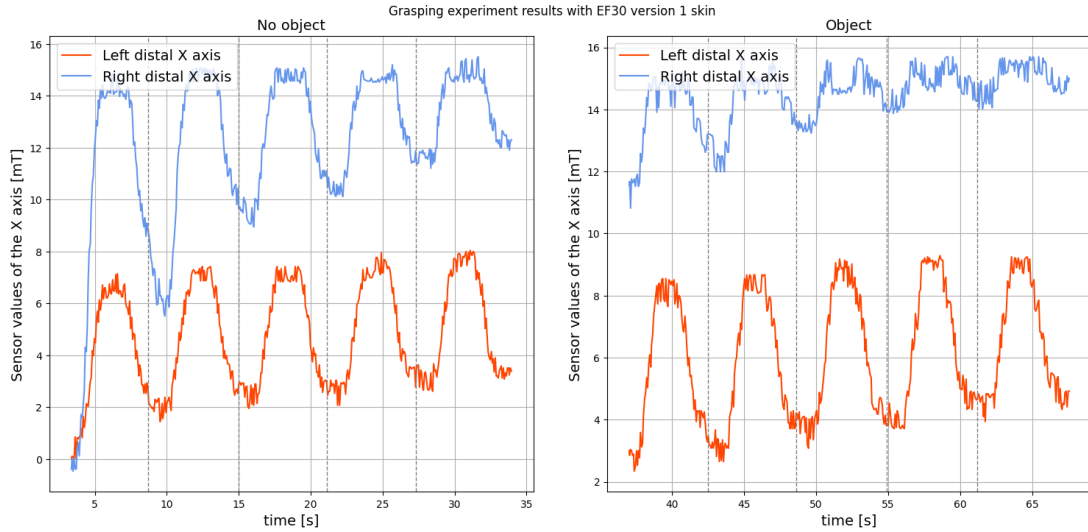


Fig. 15: *Grasping experiment time series using the EF30 version 1 of the skin. On the left is the time series without any objects, whilst on the right the object was added.*

Testing these different skins has put forwards the importance of securing the skin to the finger in order to have repeatable and therefore usable data.

3.3 Object orientation

A benefit of having sensors on both sides of the finger is its sensitivity to the direction of the force. In this grasping test, the object was slightly tilted by raising one side approximately 2 cm. Fig. 16 shows the average amplitude of five measurements, with either the left or the right side tilted. The amplitude of the sensor on the side of the tilt is significantly higher than the sensor on the opposite side.

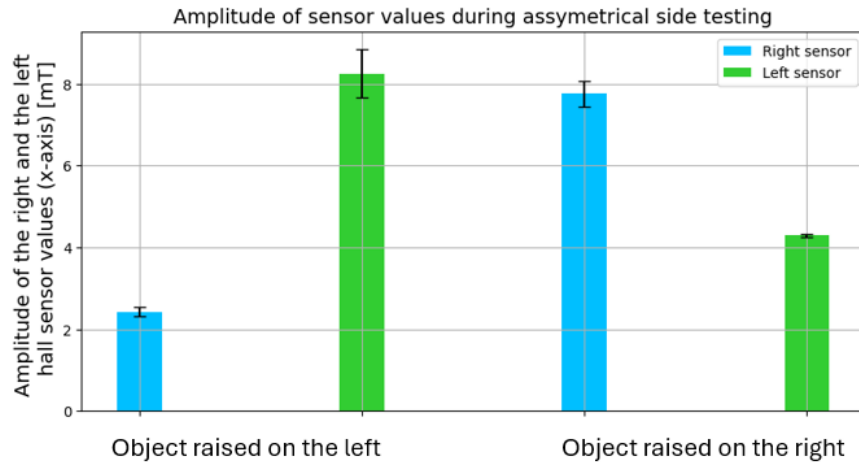


Fig. 16: *Grasping test with a tilted object, showing the average amplitude of each sensor during these tests.*

3.4 Skin sensitivity

A force test was conducted to determine the sensitivity of the finger sensors. Fig. 17 and Fig. 18 show the correlation between force and sensor values in the fingertip with two different skins: the glued and screwed EF30 and EF50 V2 skins. The results show that while both skins experience a similar force, the EF50 skin shows a lower sensitivity with peak values lower than 2mT, compared to peak values between 4 and 5mT for the EF30 skin.

Fig. 17 has 3 sensor values on its graph while Fig. 18 has only two because between these two tests the top sensor broke. Because of lack of time, it was not repaired for the EF50 test. Additionally there is an offset between the left and right sensors on Fig. 17. This was most likely caused by a slight misalignment between the finger and the scale.

While these results are not enough to allow us to infer the force based only on sensor data, they demonstrate that the sensor data is correlated with the force applied on each finger. These tests also allows us to confirm that the EF30 V2 skin is quite a bit more sensitive than the EF50 V2 skin, as we already expected from the results of the repeatability test in section 3.2.

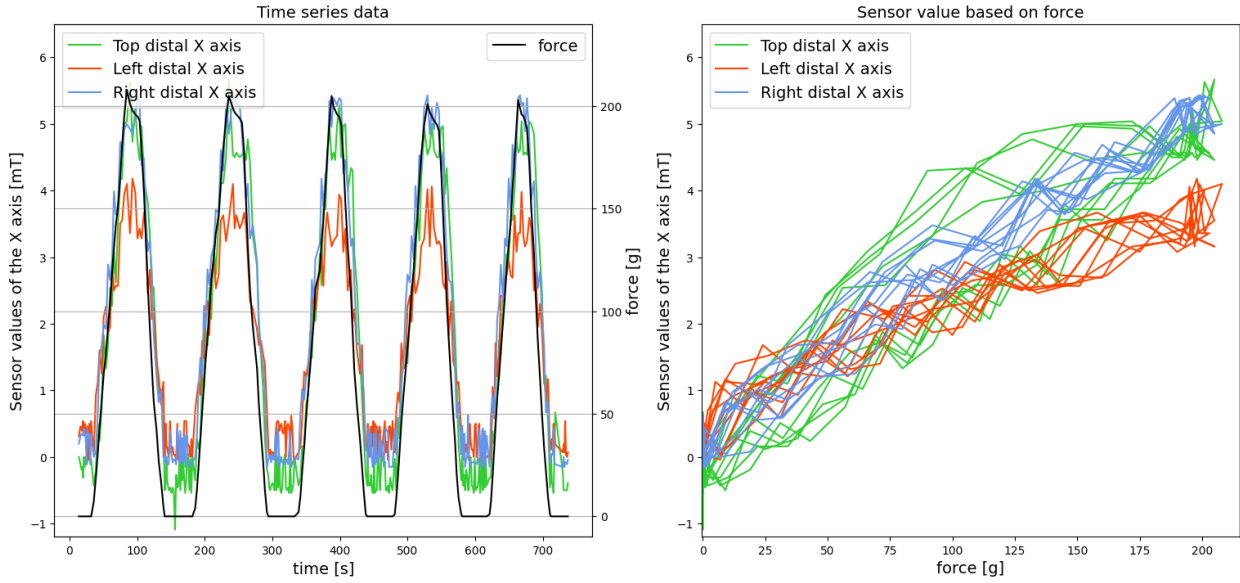


Fig. 17: *Force experiment using the EF30 skin. Left: time series plot showing the correlation between the sensors readouts (left axis), and the force (right axis). Right: Plot of the sensor values based of the force exerted on the fingertip.*

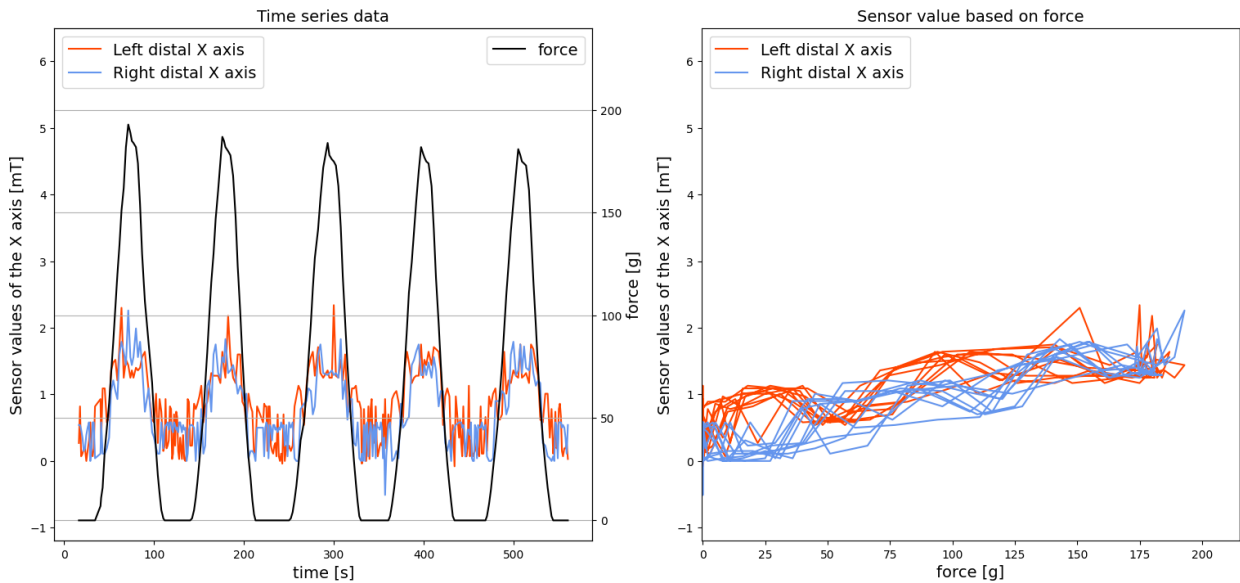


Fig. 18: *Force experiment using the EF50 skin. Left: time series plot showing the correlation between the sensor's readouts (left axis), and the force (right axis). Right: Plot of the sensor values based of the force exerted on the fingertip.*

3.5 Full hand

Due to lack of time, no experimental setup was designed for the full hand. However, after installing the PCBs, a simple visualisation code was created in order to visualise the sensor's response to the hand being touched. Fig. 19 shows images of the hand being probed (bottom image) and the corresponding sensor values, illustrated by circles proportional to the sensor values. (top image).

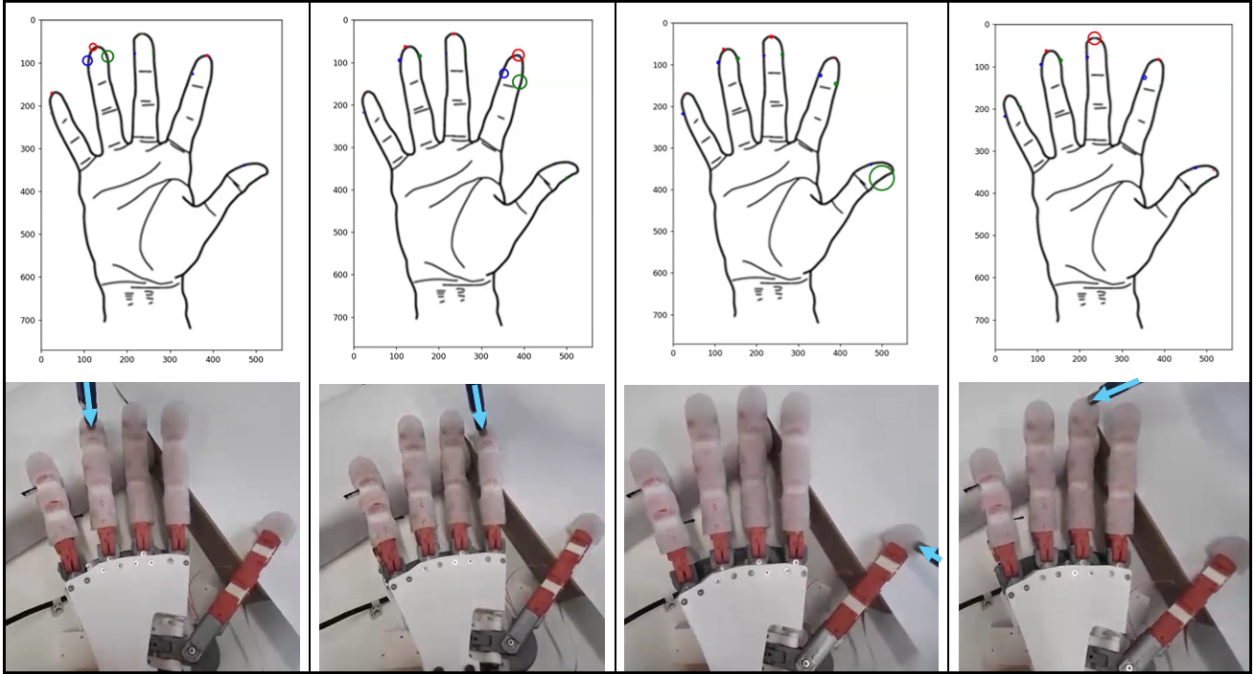


Fig. 19: Pictures of the hand being poked (bottom), and the sensor response (top). The circles on the finger are proportional to the sensor response.

4 Discussion

The results from the various tests and experiments provide several key insights into the optimal design and functionality of the force-sensing system for the robotic hand.

The UR5 test (section 3.1) proved that the entire finger can be covered by using 7 sensors. It also gave an initial idea that the sensing mechanism is dependent on the force applied.

Throughout multiple tests, the design of the finger also showed its importance. Though the V1 version was easier to design and manufacture, it proved too unreliable to function with the finger in motion. The second version with fixations in the back and glue in the front proved to be much more reliable.

Through both the repeatability test (section 3.2) and the force sensing test (sections 3.4), it was determined that EcoFlex 30 silicone (EF30) has the optimal stiffness for the skin of the robotic fingers. This silicone offers the necessary sensitivity and flexibility, ensuring that the sensors can accurately detect and measure forces applied to the skin, while avoiding disturbances from the movement of the finger.

It was also shown that the shape of the silicone skin around the finger joints also significantly impacts the repeatability and accuracy of the sensor readings. The bending motion experiment (section 3.2) demonstrates that the curved skin design around the joint prevents the silicone from bunching up too much when the finger bends. This reduces the bad readings that could be misinterpreted as a force being applied to the finger, when the finger bends. Together with a good silicone stiffness, the curved design helps ensure the decoupling of the force sensing from the movement of the finger.

The system's ability to detect the orientation of the force was validated through the sideways object experiment (section 3.3). When a force is not perpendicular to the finger, one sensor will see higher values than the other, thus allowing the orientation of the force to be determined.

The integration of magnets and hall sensor proved to be a functional method of not only object detection but also force measurements. Although more experiments need to be run to be able to determine the force based on the sensor readings, one can already tell there is a correlation between these values. By using better experimental setups, that can measure the force more precisely, in several directions and in several finger positions, we should be able to calibrate the sensors and infer the force directly from these readings.

To further enhance the tactile sensing of the hand, additional sensors should be incorporated into the palm. According to [9], the critical areas of the palm are under the pinky finger, next to the thumb and on the lower part of the palm, close to the wrist.

Beyond force sensing, it could also be useful to add other types of sensors, such as temperature or distance sensing, as this could enhance the functionality of the hand.

Given the promising outcomes demonstrated by the experiments, we are confident that this force sensing mechanism, composed of Hall sensors and magnets embedded in the skin, has a lot of potential. This approach to tactile sensing not only offers precise contact detection but could also enable accurate force measurement.

5 Bibliography

References

- [1] Andrew Belford et al. "Using Miniaturized Strain Sensors to Provide a Sense of Touch in a Humanoid Robotic Arm". In: *Frontiers in Mechanical Engineering* 6 (Oct. 19, 2020). Publisher: Frontiers. ISSN: 2297-3079. DOI: 10.3389/fmech.2020.550328. URL: <https://www.frontiersin.org/articles/10.3389/fmech.2020.550328>.
- [2] Dai-Dong Nguyen et al. "Design, Fabrication, and Validation of a Flexible Tactile Sensor for a Hand Prosthesis". In: *IEEE Sensors Journal* 24.6 (Mar. 2024). Conference Name: IEEE Sensors Journal, pp. 7222–7233. ISSN: 1558-1748. DOI: 10.1109/JSEN.2024.3359171. URL: <https://ieeexplore.ieee.org/document/10418871>.
- [3] H. Kawasaki, T. Komatsu, and K. Uchiyama. "Dexterous anthropomorphic robot hand with distributed tactile sensor: Gifu hand II". In: *IEEE/ASME Transactions on Mechatronics* 7.3 (Sept. 2002), pp. 296–303. ISSN: 1083-4435. DOI: 10.1109/TMECH.2002.802720. URL: <http://ieeexplore.ieee.org/document/1032411/>.
- [4] Wenzhen Yuan, Siyuan Dong, and Edward H. Adelson. "GelSight: High-Resolution Robot Tactile Sensors for Estimating Geometry and Force". In: *Sensors* 17.12 (Dec. 2017). Number: 12 Publisher: Multidisciplinary Digital Publishing Institute, p. 2762. ISSN: 1424-8220. DOI: 10.3390/s17122762. URL: <https://www.mdpi.com/1424-8220/17/12/2762>.
- [5] Huanbo Sun, Katherine J. Kuchenbecker, and Georg Martius. "A soft thumb-sized vision-based sensor with accurate all-round force perception". In: *Nature Machine Intelligence* 4.2 (Feb. 2022). Publisher: Nature Publishing Group, pp. 135–145. ISSN: 2522-5839. DOI: 10.1038/s42256-021-00439-3. URL: <https://www.nature.com/articles/s42256-021-00439-3>.
- [6] Byungjune Choi et al. "Development of Anthropomorphic Robot Hand with Tactile Sensor : SKKU Hand II". In: *2006 IEEE/RSJ International Conference on Intelligent Robots and Systems*. 2006 IEEE/RSJ International Conference on Intelligent Robots and Systems. Beijing, China: IEEE, Oct. 2006, pp. 3779–3784. ISBN: 978-1-4244-0258-8 978-1-4244-0259-5. DOI: 10.1109/IROS.2006.281763. URL: <http://ieeexplore.ieee.org/document/4058994/>.
- [7] David Lanigan and Yonas Tadesse. "Low Cost Robotic Hand that Senses Heat and Pressure". In: (2017).
- [8] Lorenzo Jamone et al. "Highly Sensitive Soft Tactile Sensors for an Anthropomorphic Robotic Hand". In: *IEEE Sensors Journal* 15.8 (Aug. 2015), pp. 4226–4233. ISSN: 1530-437X, 1558-1748. DOI: 10.1109/JSEN.2015.2417759. URL: <http://ieeexplore.ieee.org/document/7070742/>.
- [9] Oliver Shorthose et al. "Design of a 3D-Printed Soft Robotic Hand With Integrated Distributed Tactile Sensing". In: *IEEE Robotics and Automation Letters* 7.2 (Apr. 2022), pp. 3945–3952. ISSN: 2377-3766, 2377-3774. DOI: 10.1109/LRA.2022.3149037. URL: <https://ieeexplore.ieee.org/document/9706272/>.
- [10] *TMAG5273 data sheet, product information and support / TI.com*. URL: <https://www.ti.com/product/TMAG5273>.